UNIVERSITY OF GOTHENBURG

LICENTIATE THESIS

Far-infrared conformer-specific signatures of small aromatic molecules of biological importance

Author:
Vasyl YATSYNA

Supervisor:
Doc. Vitali
ZHAUNERCHYK

Examiner:
Prof. Dag
HANSTORP

A thesis submitted in fulfillment of the requirements for the Licentiate degree

at the

Department of Physics
University of Gothenburg

31st August, 2016

Abstract

Far-infrared conformer-specific signatures of small aromatic molecules of biological importance

by Vasyl YATSYNA

Our understanding of many biological processes requires knowledge about biomolecular structure and weak intra- and intermolecular interactions (e.g. hydrogen bonding). Both molecular structure and weak interactions can be directly studied by far-infrared (or THz) spectroscopy, which probes low-frequency molecular vibrations. In this thesis I present the results of experimental and theoretical investigations of far-infrared vibrations in small aromatic molecules of biological relevance. To enable a direct comparison with theory, far-infrared spectroscopy was performed in the gas phase with a conformer-selective IR-UV ion-dip technique. The far-infrared spectra of molecules containing a peptide (-CO-NH-) link revealed that the low-frequency Amide IV-VI vibrations are highly sensitive to the structure of the peptide moiety, the molecular backbone, and the neighboring intra- and intermolecular hydrogen bonds. The study of far-infrared spectra of phenol derivatives identified vibrations that allow direct probing of strength of hydrogen-bonding interaction, and a size of a ring closed by the hydrogen bond. Furthermore, benchmarking theory against the experimental data identified advantages and disadvantages of conventional frequency calculations for the far-infrared region performed with *ab initio* and density functional theory. For example, the conventional approaches were not able to reproduce strongly anharmonic vibrations such as amino-inversion in aminophenol. Instead, a double-minimum potential model was used for this vibration, and successfully described the experimental spectra of aminophenol. The results presented in this thesis can assist the interpretation of far-infrared spectra of more complex biomolecules, pushing forward low-frequency vibrational spectroscopy for efficient structural analysis and the studies of weak interactions.

Keywords: low-frequency vibrations, far-IR spectroscopy, hydrogen bonding, anharmonic vibrations, second-order vibrational perturbation theory

List of Papers

This thesis is based on the following papers, which are referred to in the text by their Roman numerals.

I **Aminophenol isomers unraveled by conformer-specific far-IR action spectroscopy**
Vasyl Yatsyna, Daniël J. Bakker, Raimund Feifel, Anouk M. Rijs, and Vitali Zhaunerchyk
Phys. Chem. Chem. Phys., 2016, **18**, 6275-6283

II **Far-infrared Amide IV-VI spectroscopy of isolated 2- and 4-MethylAcetanilide**
Vasyl Yatsyna, Daniël J. Bakker, Raimund Feifel, Anouk M. Rijs, and Vitali Zhaunerchyk
J. Chem. Phys., accepted for publication (August 26, 2016)

III **Far-Infrared Signatures of Hydrogen Bonding in Phenol Derivatives**
Daniël J. Bakker, Atze Peters, Vasyl Yatsyna, Vitali Zhaunerchyk, and Anouk M. Rijs
J. Phys. Chem. Lett., 2016, **7** (7), pp. 1238–1243

All the papers included in the thesis are the result of team work and international collaboration. My position in the author lists reflects the amount of work on the respective papers. In the cases when I am in the first position of the author list, I had the main responsibilities for the paper, including experimental data analysis, quantum chemical calculations and manuscript preparation. My contribution for the paper III included experimental and theoretical studies performed for ethylvanillin conformers, discussion of the methods and results, and taking part in manuscript preparation.

Also, during my PhD I have authored the following papers, but they are not included in this thesis, being out of scope of the current topic:

1 **Infrared action spectroscopy of low-temperature neutral gas-phase molecules of arbitrary structure**
Vasyl Yatsyna, Daniël J. Bakker, Raimund Feifel, Anouk M. Rijs, and Vitali Zhaunerchyk
Phys. Rev. Lett, accepted for publication (August 10, 2016)

2 **NEXAFS and XPS studies of nitrosyl chloride**
Luca Schio, Cui Li, Susanna Monti, Peter Salén, Vasyl Yatsyna, Raimund Feifel, Michele Alagia, Robert Richter, Stefano Falcinelli, Stefano Stranges, Vitali Zhaunerchyk and Vincenzo Carravetta
Phys. Chem. Chem. Phys., 2015, **17**, 9040-9048

3 **Complete dissociation branching fractions and Coulomb explosion dynamics of SO_2 induced by excitation of O 1s pre-edge resonances**
Peter Salén, Vasyl Yatsyna, Luca Schio, Raimund Feifel, Magnus af Ugglas, Robert Richter, Michele Alagia, Stefano Stranges, and Vitali Zhaunerchyk
J. Chem. Phys., 2015, **143**, 134302

4 **Experimental and theoretical XPS and NEXAFS studies of N-methylacetamide and N-methyltrifluoroacetamide**
Cui Li, Peter Salén, Vasyl Yatsyna, Luca Schio, Raimund Feifel, Richard Squibb, Magdalena Kamińska, Mats Larsson, Robert Richter, Michele Alagia, Stefano Stranges, Susanna Monti, Vincenzo Carravetta and Vitali Zhaunerchyk
Phys. Chem. Chem. Phys., 2016, **18**, 2210-2218

5 **NEXAFS spectroscopy and site-specific fragmentation of N-methylformamide, N,N-dimethylformamide, and N,N-dimethylacetamide**
Peter Salén, Vasyl Yatsyna, Luca Schio, Raimund Feifel, Robert Richter, Michele Alagia, Stefano Stranges and Vitali Zhaunerchyk
J. Chem. Phys., 2016, **144**, 244310

Contents

List of Abbreviations

IR	**I**nfra**R**ed
FIR	**F**ar-**I**nfra**R**ed
UV	**U**ltra**V**iolet
TOF	**T**ime-**O**f-**F**light
He	**He**lium
Ar	**Ar**gon
Xe	**Xe**non
FEL	**F**ree **E**lectron **L**aser
FELIX	**F**ree **E**lectron **L**aser for **I**nfrared e**X**periments
HF	**H**artree-**F**ock
MD	**M**olecular **D**ynamics
DFT	**D**ensity **F**unctional **T**heory
REMPI	**R**esonance **E**nhanced **M**ulti-**P**hoton **I**onization
VPT2	Second-order **V**ibrational **P**erturbation **T**heory

Dedicated to my family – Anna and little Sofia

Chapter 1

Introduction

1.1 Far-infrared molecular vibrations and their importance

Functionality of biomolecular systems is closely related to their three-dimentional structure. Therefore, detailed information about the structure of biomolecules is a key to our understanding of different biological processes, such as energy transfer, molecular recognition, enzyme catalysis or regulation of protein activity upon conformational changes. Infrared (IR) vibrational spectroscopy in combination with modern quantum-chemical calculations is one of the methods which can reveal molecular structural information at the atomic level of detail, and probe intra- and inter-molecular interactions directly. This is due to the fact that molecular vibrations are strongly dependent on both the strength of covalent bonds, and the electrostatic environment around the vibrating groups of atoms.

The frequency region of the so-called mid-IR light is typically defined as 800-4000 cm^{-1} (12.5-2.5 μm). Mostly localized vibrations are excited in the mid-IR range, carrying information about local structural arrangement of vibrating atoms. Far-infrared (or TeraHertz) light, which the current thesis focuses on, covers the range below 800 cm^{-1}. Delocalized vibrations, or local vibrations with very low force constants are excited in the far-IR range. Far-IR vibrations typically have high degree of anharmonicity and mode-coupling, and are strongly sensitive to the large-scale molecular structure and shape. Moreover, the far-IR range contains vibrations directly associated with weak interactions important in biological molecules, such as hydrogen bonding and dispersion forces (e.g. π-π and XH$\cdots\pi$ interactions). These unique features of the far-IR range make far-IR spectroscopy a highly suitable tool for structural analysis of large

and flexible biological molecules. Until recently, the application of far-IR spectroscopy for structural analysis has been hindered by several obstacles. First, it requires powerful light source as the absorption cross-sections of far-IR vibrations are typically low. And second, theoretical predictions of far-IR vibrations and spectra are complicated by a high degree of anharmonicity and mode-coupling, thus making the structural assignment very challenging. However, both these limitations have recently been liberated: the first one thanks to the emergence of powerful far-IR light sources such as free electron lasers [1] and table-top single-pulse THz sources; the second one thanks to the advance of computing facilities, and the development of powerful quantum-chemical models and molecular dynamics simulation approaches [2–4]. Still, the far-IR region remains quite unexplored, and its application for structural analysis of increasingly large biological systems requires in-depth understanding of far-IR spectra of smaller biological building blocks. Thus, this thesis is devoted to the far-IR signatures of small aromatic molecules of biological importance, which can be studied in a conformer-specific manner in the gas-phase, and combined with highly accurate quantum-chemical calculations.

1.2 Molecular structural analysis based on IR spectra and quantum-chemical calculations

Many molecules, especially biomolecules, have the property of conformational isomerism. This means that the molecules having the same chemical formula and the same sequence of bonded atoms can exist in very different three-dimensional structures. These structures, also called conformers, can typically be interconverted between each other by means of various rotations about the bonds. Each molecular structure has its distinct force fields for atomic motions, and hence different vibrational frequencies. Thus, in principle, the different structures can be identified by means of vibrational spectroscopy using IR light sources. The frequencies of the molecular vibrations are very sensitive to the strength of the bonds involved in the atomic motions, and both intra- and inter-molecular interactions. This allows in-depth studies of both intrinsic structure of molecules, as well as the effect of the neighboring environment.

Even though each molecular vibration carries information about the local and/or global structural arrangement of atoms, the precise molecular structural analysis is typically not possible without quantum-chemical calculations. Within harmonic approximation, the number of vibrational normal modes, i.e. the characteristic vibrations of polyatomic molecule, is determined by $3N$-6 ($3N$-5 for linear molecules), where N is the number of atoms. This means that even for relatively small molecule such as amino-acid alanine, having 13 atoms, there are 33 characteristic vibrations, each having a certain distinct frequency and type of atomic motion. Qualitative information, such as the relative strength of certain bonds, can be obtained from experimental spectra. Information for precise structural arrangement, however, requires quantum-chemical computations. They can be used to predict possible geometries the molecule can adopt (conformations), their relative energies, and can be used to calculate the corresponding IR spectra. The structural assignments then can be based on a comparison between the experimental and theoretical IR spectra.

Gas-phase studies of molecular vibrations have several advantages in contrast to the condensed phase. First, they enable direct comparison of experimental data with computer simulations performed on isolated systems. Second, they provide a direct exploration of intrinsic properties of the molecules without influence of interactions with the surrounding solvent or crystalline environment. Third, when deep understanding of vibrational signatures of gas-phase (bio)molecules is obtained, this knowledge can be applied for the analysis of more complicated spectra obtained in natural environments. Mid-IR spectroscopy in the gas-phase, combined with theoretical calculations was very successful in structural analysis of many molecules of biological interest [5–7], even up to systems as large as the pentadecapeptide gramicidin [8] and decapeptide Gramicidin S [9, 10]. A very good extension to the mid-IR range is far-IR spectroscopy, a key topic of this thesis, studying non-local anharmonic vibrations that are very sensitive to both local and global molecular structures.

Fig. 1.1 illustrates the strength of the combination of far-IR spectroscopy and quantum-chemical calculations. It shows experimental gas-phase far-IR spectra measured by us for two different conformers of the ethylvanillin molecule. The right side of the figure contains stable structures (conformers) that ethylvanillin

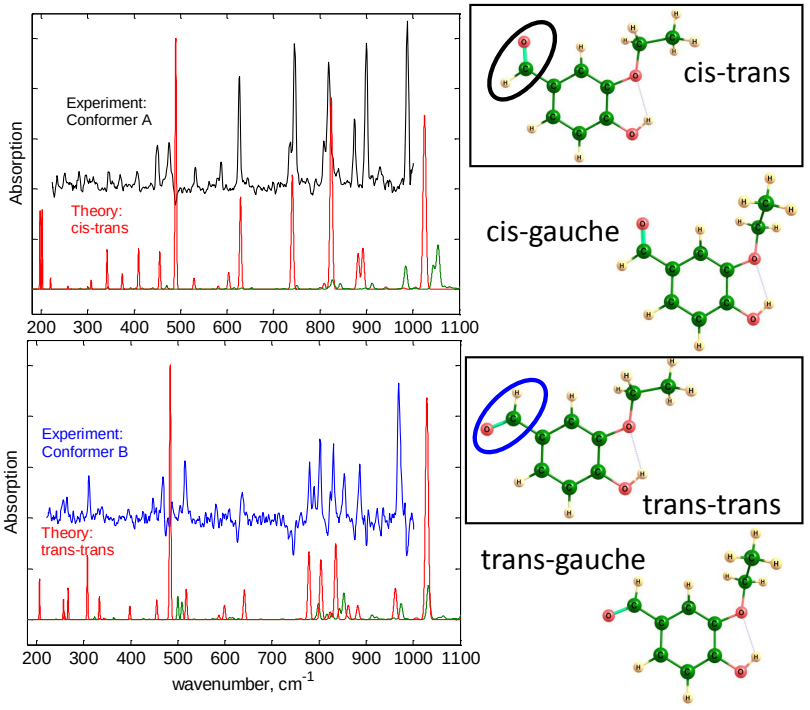

FIGURE 1.1: Comparison between the experimental and calculated spectra of ethylvanillin conformers (left), together with the possible structures this molecule can adopt (right). The structures of the assigned *cis-trans* and *trans-trans* conformers are highlighted with rectangles.

can adopt in the gas phase, obtained by means of a geometry optimization algorithm and density functional theory. The vibrational frequencies and intensities for each conformer were computed as well, yielding the theoretical IR spectra. Comparison between the experimental and calculated spectra strongly favors the assignment of the conformers A and B to the *cis-trans* and *trans-trans* structures, respectively. It is worth noting that these two conformers have only a minor difference in their structure: their aldehyde functional group (O=C-H) is rotated by 180 degrees around the C-C bond with respect to another conformer. Such alternation of the molecular geometry only slightly changes the arrangement of masses within the molecule, but nevertheless the experimental and theoretical IR spectra show significant differences between them.

1.3 Computational spectroscopy: treatment of anharmonic vibrations

1.3.1 Quantum chemical computations in general

In quantum chemistry the principles of quantum mechanics are used for the description of different physical and chemical properties of the molecules. If theoretical principles are solely used in the calculations, with no empirical parameters or experimental data, such quantum-chemical methods are called *ab initio*. Most of the quantum chemical methods rely on the solution of the Schrödinger equation with a molecular Hamiltonian that describes the electrons and nuclei of the molecules. The well-known Hartree-Fock (HF) [11] approach is one of such methods. Certain approximations have to be applied, as the exact solution of the Schrödinger equation is not possible for systems larger than the hydrogen atom. The most important is the Born-Oppenheimer approximation [12], where the motion of electrons and nuclei are treated separately. It enables the separation of electron and nuclei coordinates, and allows solving the Schrödinger equation in two steps. In this way the potential energy of the molecule versus the positions of nuclei, a potential energy surface, can be calculated. This allows performing molecular geometry optimizations, which can find the equilibrium structures corresponding to different potential energy minima on this surface. Second-order energy derivatives in the vicinity of the potential energy surface minima yield vibrational properties of molecules.

Density functional theory (DFT) is different from the wave-function methods, such as HF, and relies on the principle that the energy of the molecular system is completely determined from the electron density. For the HF method, however, the energy depends on the wave-function of the many-body system. The wave-function in this case describes the probability amplitude of a many-body system, and is a solution of the many-body Schrödinger equation. In the DFT methods the spatial electron density carries all the information about the system. For example, dips in the electron density give the positions of the nuclei, while the magnitude of the dips gives nuclei charge. The energy of the system is approximated by means of a functional, i.e. function of a function, which relates the electron density to the energy of the system. So, different DFT methods vary by the choice of such functional. The major advantage of DFT methods is a favorable

scaling of the computational cost versus the number of atoms (electrons), allowing accurate calculations for large systems at relatively low computational cost. DFT is the main quantum-chemical method used in this thesis.

1.3.2 Treatment of vibrational anharmonicity

In the literature, the assignment of experimental IR spectra is typically based on quantum chemical calculations (e.g. with DFT) where geometry optimizations and subsequent vibrational analysis in the double harmonic approximation are performed. The major goals of these calculations are to identify conformations contributing to the experimental spectra and to reveal detailed information about the forces which determine the structure of the conformers. Within the double harmonic approximation the potential energy surface and dipole moment are truncated at the second and first order respectively, usually leading to overestimated vibrational frequencies and less accurate intensities. To overcome this drawback, different scaling methods for harmonic frequencies (or force field) have been proposed [13–17], and are widely used to correct the band positions of the fundamental transitions. However, this approach is usually not suitable for the low frequency region due to anharmonic mode couplings. Furthermore, it does not give any information about the intensities of overtones and combination bands, which might be important for a correct analysis of experimental IR signatures.

There are several generally applicable methods which go beyond the harmonic approximation, and they can be divided into dynamical (time-dependent) approaches, such as *ab initio* molecular dynamics (MD) simulations [2–4], and time independent approaches, with most effective implementations built on second order-vibrational perturbation theory (VPT2) [18–20], and vibrational self-consistent field (VSCF) approach [21]. *Ab initio* MD simulations are based on a classical treatment of the nuclei, and quantum mechanical treatment of the electrons, *e.g.* with DFT formalism [3]. The dynamics simulations are performed at finite temperatures and therefore they naturally describe conformational dynamics, as well all anharmonic effects due to sampling of all accessible parts of the potential energy surface. Despite large computational cost, this approach is particularly appealing when available experimental spectra are obtained at room temperatures, and hence contain natural broadening of the lines

due to all populated conformations. It was also shown to be very successful in describing gas-phase far-IR spectra of peptide systems with large number of torsional degrees of freedom [22, 23].

Time independent VSCF computations are based on the approximation that each vibrational mode is moving in the mean field of the rest of the vibrational motions. The total wave function of the VSCF approximation is a product of single mode wave functions, which are determined self-consistently. The VSCF approach was successfully applied to large systems of biological interest [21], despite a problematic description of strongly coupled vibrational modes and higher excited states due to correlation effects between the different modes. Correlation corrected modifications of the VSCF method (such as VSCF-PT2) increase the accuracy of the calculated vibrational transitions, but are limited to medium sized molecular systems on the order of 20-30 atoms [24], due to an increased computational cost.

In this thesis the anharmonic treatment of far-IR vibrations is based on the vibrational second-order perturbational (VPT2) theory [18–20]. The VPT2 method was shown as a reliable tool for the prediction of fundamental vibrational transitions, as well as first overtones and combinational bands. It is considered to be especially effective for semi-rigid, isolated molecular systems [20], and most of the molecules studied in this thesis can be considered as such. It should be noted, however, that the evaluations of the VPT2 approach [20] focused on the mid-IR region, while the far-IR vibrations were not always included due to lack of experimental data. In this thesis such evaluations have been performed, as our experimental data were obtained in a conformer-selective manner, and under isolated gas-phase conditions. This allows direct comparison with the results of *ab initio* calculations that are typically performed for isolated molecules in a single conformation.

1.4 Molecular systems investigated

1.4.1 Aminophenol isomers

Aminophenol molecule exists in a form of three isomers (see Fig. 1.2), which differ by the location of the NH_2 group with respect to the OH group, and are named as ortho- (2AP), meta- (3AP) and para- (4AP) aminophenol. In addition, the 3AP and

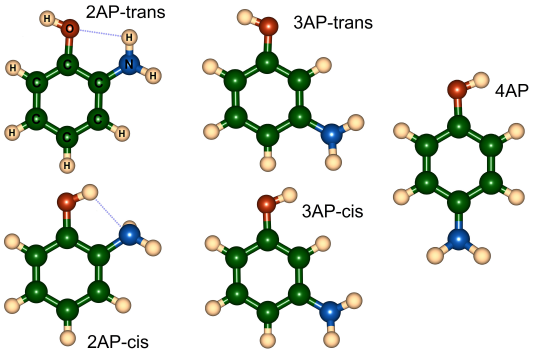

FIGURE 1.2: Optimized geometries of aminophenol isomers, namely 2AP (*trans* and *cis* conformers), 3AP (*trans*, *cis*), and 4AP. The hydrogen atoms of the amino-group (NH_2) are positioned out of plane with respect to the aromatic ring. Geometry optimization was performed with the B3LYP/aug-cc-pVTZ method.

2AP molecules exhibit rotational isomerism for different orientations of the OH group with respect to the NH_2 group. This leads to the distinct *trans* and *cis* conformers. Also, the intra-molecular hydrogen bond of NH$\cdots$O or OH$\cdots$N types can exist for 2AP conformers due to the close adjacency of the hydroxyl- and amino- functional groups. It is worth noting that the aminophenol isomers can also be considered as aniline or phenol derivatives, where the hydrogen atoms are substituted by hydroxyl- and amino- groups, correspondingly, in corresponding position of the phenyl ring. Such substitutions change the physical and chemical properties of the substituted molecules, including the vibrational structure.

1.4.2 MethylAcetanilide molecule as a peptide model

The peptide link, -CO-NH-, is one of the main structural units of a protein or peptide, as it connects two consecutive amino-acids in the protein chain. The MethylAcetanilide (MA) molecule, studied in this thesis, can be considered as a simple peptide model with one peptide link. The peptide link in MA connects a methyl group with a substituted aromatic ring (methylphenyl group). Two different isomeric configurations of MA were studied, 2-MA and 4-MA (see Fig. 1.3).

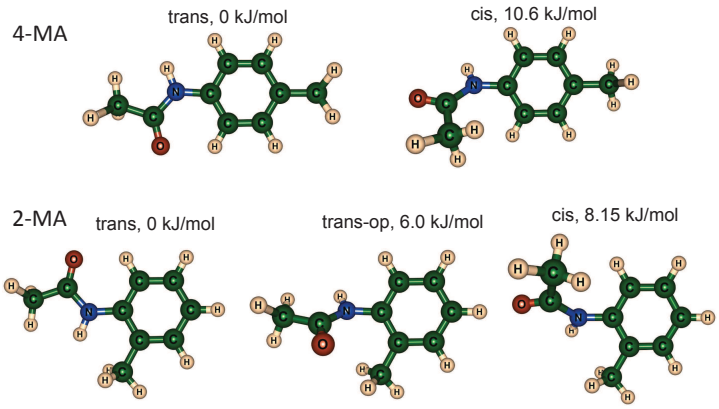

FIGURE 1.3: Optimized geometries and corresponding energies of the stable conformations of 4-MethylAcetanilide (4-MA) and 2-MethylAcetanilide (2-MA), calculated with the B3LYP density functional and N07D basis set. The energy of the conformations is shown with respect to the *trans* ones.

The -CO-NH- moiety can exist in two distinct nearly planar configurations, either *trans* or *cis*. In the case of 4-MA, this results in two geometries (see Fig. 1.3), which have a significant difference in energy. In the case of 2-MA, where the substituent methyl group is adjacent to the acetamide group, steric interactions lead to the presence of the third conformer, with the -CO-NH- moiety of *trans* character, but oriented out of plane with respect to the aromatic ring. This conformation has a non-zero dihedral angle ($\approx 60°$) between the -CO-NH- moiety and the ring planes, and we call it *trans-op* 2-MA. Moreover, for this conformation the -CO-NH- moiety deviates from planarity by $\approx 10°$ (B3LYP/N07D geometry). The influence of this structural feature on the far-IR vibration is particularly interesting, as deviation from planarity is quite common in proteins [25, 26].

1.4.3 Phenol derivatives with intra-molecular hydrogen bonding

The phenol derivatives studied, shown in Fig. 1.4, were chosen for their capacity to form intra-molecular hydrogen bonds, as well as for their ability for resonant absorption of UV photons, allowing us to study them in a conformer-specific manner. The chatecol and saligenin molecules exists in a single conformation,

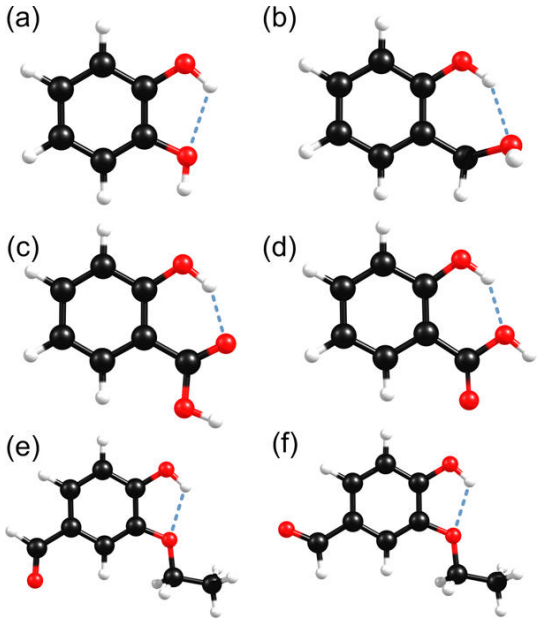

FIGURE 1.4: The structures of studied phenol derivatives in their observed conformations: cathecol (a), saligenin (b), rotamer 1 (c) and rotamer 2 (d) of salicylic acid, conformers cis-trans (e) and trans-trans (f) of ethylvanillin. Carbon atoms are depicted with black spheres, oxygen - with red, and hydrogen with white.

while for salicylic acid and ethylvanillin two conformations for each molecule were observed. For the saligenin molecule, the rotamer 1 and rotamer 2 differ by a rotation around the C-C bond of the carboxylic acid group (see Fig. 1.4c,d). For ethylvanillin, the *cis-trans* and *trans-trans* conformations differ by the rotation around the C-C bond of the aldehyde group (see Fig. 1.4e,f).

Intra-molecular hydrogen bonds are present in all the conformations studied. Six-membered rings are formed by a hydrogen bond in the cases of saligenin and salicylic acid, and five-membered rings in the cases of cathecol and ethylvanillin. Far-IR vibrations, which deform the hydrogen-bonded parts of the molecules, are expected to give direct information about the hydrogen-bond interaction.

Chapter 2

Methods

In this chapter I will describe briefly the experimental techniques and the computational approaches applied in this thesis. First, a general overview of the experimental setup is presented, followed by the methodology for the cooling of molecules in the gas-phase. Second, the method for conformer selection by means of the REMPI technique is described. Third, the IR-UV ion-dip spectroscopy is described, which is a key experimental technique for the far-infrared experiments presented in this work. Finally, the computational approaches for the description and assignment of the experimental spectra are briefly described.

2.1 Experimental setup

The experiments performed in this thesis aim at measuring conformer-specific (far-)IR spectra of isolated gas-phase molecules. For this, as a first step, target molecules are delivered into gas phase (vacuum) and cooled down to cryogenic temperatures. Then, the molecules in certain conformation are selectively ionized with a resonant UV laser by means of the REMPI technique (see section 2.3), creating a constant ion signal. Just before ionization, an IR laser interacts with the molecules. If the wavelength of the IR laser is resonant with one of the molecular vibrational transitions, the ion signal is reduced. By means of scanning the wavelength of the IR laser, (far-)IR absorption spectra of a certain molecular conformer can be measured. Thus, the IR spectra of every conformer present in the gas-phase can be measured separately, by selecting the corresponding conformer-specific UV transitions.

The scheme of the experimental setup is shown in Fig. 2.1. The setup comprises three differentially-pumped vacuum chambers. In the source chamber the target molecules are delivered

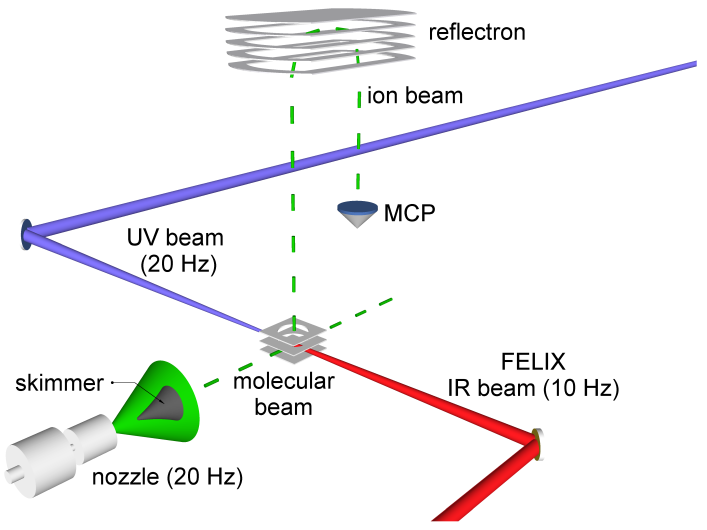

FIGURE 2.1: The scheme of experimental setup for conformer-specific infrared spectroscopy of isolated molecules cooled in a supersonic-jet expansion.

into vacuum, by means of supersonic-jet expansion of the carrier gas seeded with target molecules. In the interaction chamber the cooled molecules in a form of a molecular beam can interact with IR and UV laser beams. In the detection chamber, represented by a time-of-flight tube, the ionized molecules are detected and mass-analyzed. To achieve high vacuum conditions, the source chamber is pumped by a 1250 l/s turbo-pump (TPH 1201 UP, Pfeiffer Vacuum), while the interaction and detection chambers are pumped by 210 l/s turbo-pumps (TMH 261, Pfeiffer Vacuum) each. A diaphragm backing pump (MVP 055-3, Pfeiffer Vacuum) is used to keep the chambers dry and oil-free.

As most of the samples studied were low-volatile, a heatable molecular beam source is employed to deliver molecules into the gas phase. It consists of a resistively heated sample compartment and heated pulsed nozzle (Parker general valve Series 9). The sample compartment can be heated up to 180°C. The pulsed nozzle is kept 5-10 °C higher than the sample compartment in order to avoid condensation of the molecules on the nozzle aperture. The carrier gas (typically He or Ar at 3 bar)

passes through the heated sample compartment, capturing vaporized sample molecules. The gas together with the sample molecules is expanded into the source chamber kept under high vacuum ($\sim 10^{-7}$ mbar). After the supersonic-jet expansion the molecules pass through a skimmer ($\varnothing$=1 mm) 3.5 cm downstream the nozzle. This selects the coldest part of the expansion, and forms a collimated molecular beam that enters the interaction chamber. Here, the molecules interact with both a (far-)IR beam, produced by the Free Electron Laser for Infrared eXperiments (FELIX) [1], and with a UV beam. The latter is produced by a tunable frequency-doubled dye laser from Radiant Dyes (Narrow Scan) pumped by a pulsed YAG laser (Spectra Physics, Quanta-Ray Pro). The repetition rates of the UV and IR light pulses are 20 Hz and 10 Hz, respectively, allowing IR on/off measurements to correct for the fluctuations in the molecular source output and long-term variations in the UV light power.

As will be shown in sections 2.3 and 2.4, REMPI and IR spectra are recorded by measuring the appearance of an ion signal, or the appearance of ion signal variations. The ions are created by irradiating the neutral molecules with resonant UV laser pulses, and are detected with a time-of-flight (TOF) tube of reflectron-type [27] (Jordan TOF Products). Such detection allows recording wavelength-dependent, high resolution mass spectra of all ionized molecular species present in the molecular beam. The principle of the TOF detection is the following. Ion pulses are generated between the two grids, called extractor and repeller. A high voltage is applied to the repeller grid ($\sim$3500 V), while the extractor grid is kept $\sim$1000 V lower. The positive ions are pushed towards the TOF tube by the potential between the repeller and extractor grids. They enter the acceleration region, where they are further accelerated by the potential between the extractor plate and the grounded grid. The accelerated ions then enter the field-free region of the TOF tube where the ions are dispersed according to their mass to charge ratio, m/z. At the end of the TOF tube an ion mirror called reflectron is placed, which consists of several plates producing a retarding potential. Here the ions are reflected and propagate towards the micro-channel plate detector, thus passing a larger distance than the actual length of the TOF tube, leading to an increased mass resolution. Moreover, the reflectron compensates for the initial spread of the kinetic energy of the created ions, further increasing the mass resolution. The TOF tube used for the experiments described in this thesis

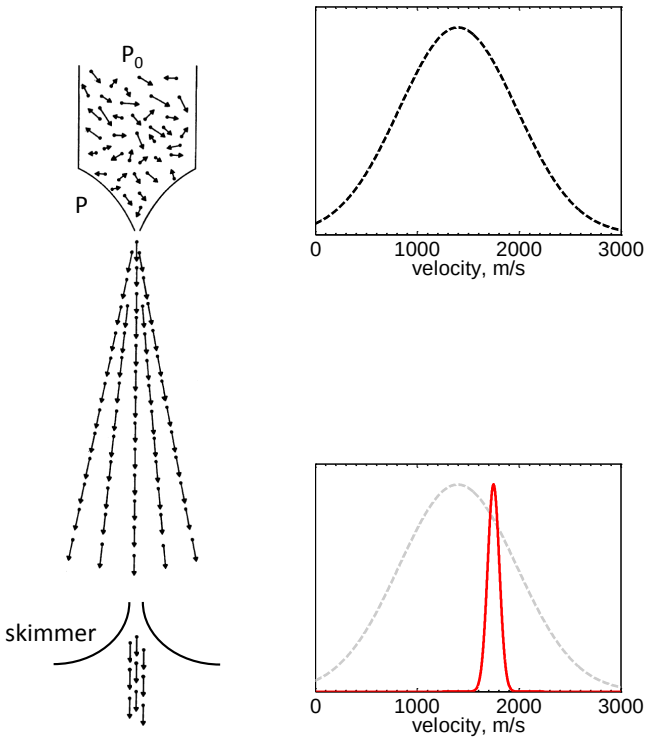

FIGURE 2.2: Schematic representation of a supersonic-jet molecular beam. Shown on the left is expansion of the gas through a nozzle from the reservoir at high pressure P_0, into the vacuum chamber kept at much lower pressure P. The skimmer selects the coldest core part of the expansion. Shown on the right is narrowing of the molecular velocity distribution due to selection of molecules with a large velocity component in the axial direction of the nozzle. The figure is adapted from Ref. [28].

allows measuring mass spectra with a mass resolution $m/\Delta m$ larger than 2000.

2.2 Supersonic-jet cooling

In order to allow for a precise structural characterization of gas-phase molecules based on their IR spectra, the spectra have to be free from features which may complicate vibrational assignment, such as hot bands and rotational broadening. In the molecular

beams prepared by supersonic-jet expansion such complications are eliminated, as the molecules are cooled down to cryogenic temperatures (< 100 K). At these temperatures only the vibrational ground state and the lowest rotational states are populated. As a result, the transitions from vibrationally excited states (hot bands) are not observed. Also, rotational contours of the vibrational transitions are usually negligible leading to narrow vibrational bands. Moreover, in cases where the molecular species can exist in several conformations, the supersonic-jet cooling allows conformer-specific IR spectra measurements (see sections 2.3 and 2.4). Apart from cooling, the supersonic-jet expansion allows delivering isolated molecules into the interaction region. It enables studying molecular properties, free from perturbations from inter-molecular interactions. Alternatively, if the inter-molecular interactions are the key objects of study, the molecular associates (clusters) can be prepared and investigated.

A detailed description of the supersonic-jet cooling and its properties is given elsewhere [28–30]. Briefly, the reservoir with gas at relatively high pressure P_0 is used, having a small orifice or shaped nozzle with diameter D. The gas from the reservoir can penetrate through the nozzle into the expansion volume with background pressure P, much lower than P_0. If the pressure in the reservoir is high enough, the mean free path of the molecules is smaller than D, so only molecules having a large velocity component in the axial direction of the nozzle escape the reservoir (see Fig. 2.2). This leads to a drastic reduction of the velocity distribution width and hence the translational temperature. The vacuum pumps are used in order to maintain the background pressure downstream the nozzle when the gas is flowing. Also, the flow of the gas can be collimated with a carefully-manufactured conical-shaped aperture (skimmer), which allows the selection of the coldest core part of the expansion region and creation of a supersonic molecular beam. Typically, noble gases such as He, Ar, or Xe at high pressure (2-10 bar) are used as a carrier gas, while the sample molecules are seeded into the gas flow by means of thermal evaporation, or by laser desorption [5, 31] for low-volatile or thermolabile molecules.

The temperature, pressure, density, and Mach number in the expansion region relate to each other according to thermodynamic laws, if desirable conditions for isentropic expansion are preserved (no viscous forces, shock waves, and heat sources or sinks such as chemical reactions etc.) [29]. The Mach number is

defined as the ratio of the flow velocity u to the local speed of sound. For an ideal gas these relations are given by

$$T/T_0 = (P/P_0)^{(\gamma-1)/\gamma} = (\rho/\rho_0)^{\gamma-1} = [1+(\gamma-1)/2M^2]^{-1}, \quad (2.1)$$

where T, P and ρ are the temperature, pressure and density in the isentropic part of the expansion, and T_0, P_0 and ρ_0 are the temperature, pressure and density in the gas reservoir, respectively. γ is the heat capacity ratio $C_p/C_v > 1$, and M is the Mach number. As it can be seen from the Eq. 2.1, since $P_0 >> P$, the translational temperature of the gas in the expansion decreases significantly.

For continuous gas flow at the distances larger than a few nozzle diameters downstream the nozzle the Mach number is given by [29]

$$M = A(x/D)^{\gamma-1}, \quad (2.2)$$

where x is the distance from the nozzle, and A is a constant which depends on γ. For monoatomic gases A equals to 3.26. As an example, according to Eq. 2.2, the Mach number of 44 and the temperature of 0.5 K can be achieved at a distance of 50 nozzle diameters downstream. Typically, by supersonic-jet cooling translational temperatures of less than 2 K are obtained [29, 30]. As the velocity distribution is very narrow at such temperatures, the energies of the collisions in the supersonic jet will be characterized by low temperatures as well. Therefore, the internal degrees of freedom, i.e. rotational and vibrational, will be equilibrated to the same low temperatures by means of low-energy collisions. However, as such equilibration requires larger propagation distances from the nozzle, where the density of the molecules and hence the probability of collisions is lower, the rotational and vibrational degrees of freedom may not reach equilibrium with translational temperature of the molecule. Reaching the rotational-translation equilibrium is a rapid process, so the rotational temperatures of 3-10 K are normally achieved [28, 29]. The vibrational cooling is less efficient and largely depends on the vibrational structure, but still results in significant depopulation of the vibrationaly excited states. Under favorable conditions typical vibrational temperatures of 10-20 K are achieved, and in most cases temperatures are below 50 K.

2.3 REMPI spectroscopy

REMPI stands for Resonance Enhanced Multi-Photon Ionization, and the associated spectroscopic technique is schematically described in Fig. 2.3. The absorption of two photons is used to excite the gas-phase molecules above the ionization potential, through an intermediate electronically excited state. The presence of a resonance in form of such an intermediate excited state enhances the absorption cross section and the ionization yield. The two photons can either have similar wavelengths or different wavelengths, which results in either one-color (1+1), or two-color (1+1') REMPI schemes, respectively. REMPI spectroscopy typically requires that the target molecule/species have a UV chromophore, which in this thesis is always an aromatic phenyl ring. The intermediate state in this case is a first electronically excited singlet-state (S_1), excited from the ground state (S_0). For the phenyl ring the S_1 excited state is relatively long-lived, resulting in sharp absorption peaks, and enabling the absorption of the second photon for ionization of the molecule. Moreover, the $S_0 \rightarrow S_1$ transition for a phenyl ring has a large oscillator strength, making REMPI spectroscopy an efficient and sensitive tool to study aromatic molecules.

REMPI spectra are typically recorded in the vicinity of the origin ($S_0 \rightarrow S_1$) transition with the help of a dye laser, producing frequency-tunable UV radiation. The origin transition is usually the strongest one in the REMPI spectrum and is denoted as "0-0" meaning that the electronic transition takes place between the states in their vibrationally ground states. Transitions with frequencies above the origin are vibronic transitions, resulting in the electronically- and vibrationally-excited molecule. REMPI spectra can also contain transitions with frequencies below the origin, which are named hot bands and result from transitions from vibrationally excited ground state. Hot bands appear when molecules are not cold enough, because then some vibrational levels of the electronically ground state can be populated. Despite the fact that hot bands complicate REMPI spectra, they can give some extra information. For example, the vibrational temperature of the molecules cooled in a supersonic-jet expansion can be estimated using the ratio between the integrated intensity of the origin band and the hot band.

REMPI spectroscopy is a very powerful method to distinguish between different conformers (rotational isomers) of the

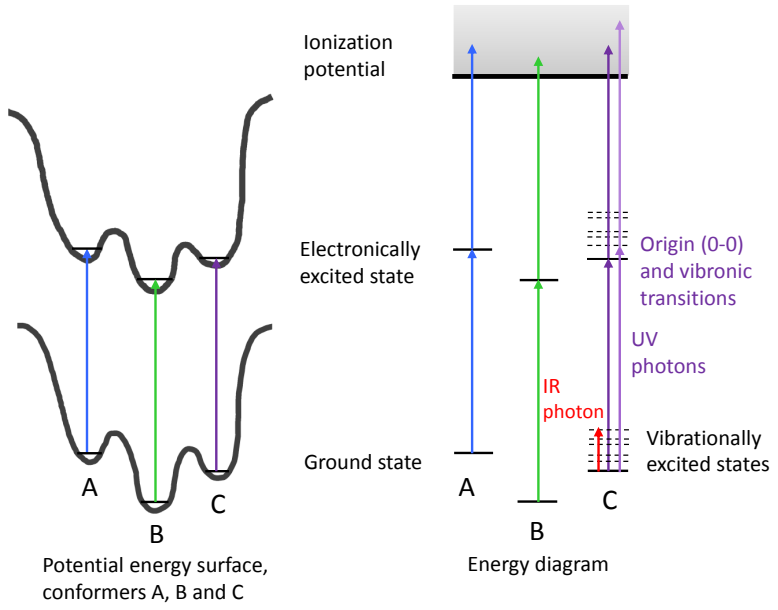

FIGURE 2.3: Schematic description of the REMPI spectroscopy technique. Shown on the left is a potential energy surface for the cooled molecules existing as three distinct conformers A, B, and C. REMPI spectroscopy probes the electronically excited states of the conformers, using the photon energies which are slightly different for the different conformers, thus allowing conformer-specific studies. In this technique two photons are absorbed leading to ionization of the molecule (shown on the right).

same molecule, as the origin 0-0 transitions of different conformers typically have slightly different frequencies. Moreover, the spectral pattern of vibronic transition can be very different for different conformers thus allowing their identification. As an illustration, Fig. 2.4 shows the REMPI spectrum of the 3-aminophenol molecule, studied in this thesis, which exists in the form of *trans*- and *cis*- isomers. First, as it can be seen from the figure, there are two strong origin transitions, each for every conformer. The red-most transition at 34118 cm^{-1} is due to the *cis* conformer, and the strongest transition to the blue, at 34476 cm^{-1}, is due to the *trans* conformer. Below the origin of the *trans* conformer (< 34476 cm^{-1}), the vibronic transitions of the *cis* conformer are observed.

It can be seen from Fig. 2.4 that the different conformations of 3-aminophenol can be excited and ionized selectively, by using different UV wavelengths of a dye laser.

With the help of two different tunable UV lasers one can also determine which peaks in the REMPI spectra are due to the same conformation. This is achieved by means of UV-UV depletion and UV-UV hole-burning methods [31]. The pulses from two lasers subsequently interact with the molecules, having a constant short time delay between each other. The laser which is first interacting with the molecules is called the pump laser, and the second is called the probe laser. In the UV-UV depletion method the frequency of the probe laser is set to match the REMPI transition of one of the conformers, hence producing a constant ion signal. The frequency of the pump laser is scanned. When the frequency of the pump laser is resonant with the vibronic transition of the probed conformation, the population of its ground state is depleted, leading to a reduction of the ion signal produced by the probe laser. In this way the REMPI peaks coming from the same conformation will be identified. In the same manner UV-UV hole-burning spectroscopy is applied, with the only difference that in this case the pump laser is fixed to the REMPI transition of one of the conformers, while the probe laser is scanned. In this case the REMPI spectrum is measured in which the peaks

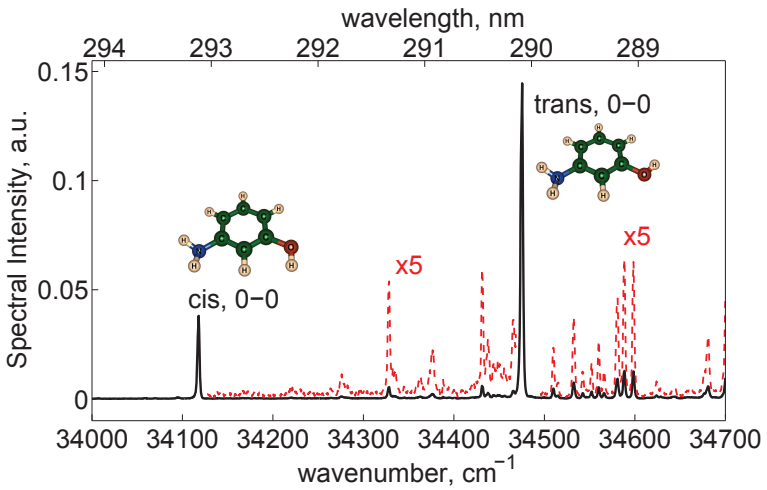

FIGURE 2.4: REMPI spectrum of 3-aminophenol. The origin transition peaks for *trans* and *cis* conformers are denoted with "0-0".

originating from the pumped conformer are removed.

A last aspect which needs some consideration here is the cooling of the molecules. If no cooling is applied, the vibrational and rotational states of the gas-phase molecules are populated which leads to very broad UV transition peaks, which are far from being resolved sufficiently to distinguish between the different conformers. That is why the supersonic-jet cooling of the molecules, leading to very low vibrational and rotational temperatures, is so important.

2.4 IR-UV ion-dip spectroscopy

IR-UV ion-dip spectroscopy, which was first demonstrated by Lee and co-workers in 1988 [32], is a key technique in this thesis. It allows the measurements of conformer-specific (far-)IR spectra of gas-phase molecules cooled by supersonic-jet expansion. The principle of this method is illustrated in Fig. 2.5. The frequency of the UV laser is tuned to match a REMPI transition of the specific molecular conformer under investigation, thus creating a constant conformer-specific ion signal. Prior to the UV laser pulse, the molecules are irradiated with (far-)IR photons from a tunable (far-)IR laser. If the frequency of the IR laser is resonant with one of the vibrational transitions of the selected conformer, the population of the ground state is depleted, thus leading to a reduced ion signal. Such ion signal variations are measured while scanning the IR laser frequency, providing an absorption IR spectrum of the selected conformer. Individual IR spectra for all conformations present in the molecular beam can be recorded in the same way by selecting their distinct REMPI transitions with a UV laser and scanning the IR wavelength.

The principle of the IR-UV ion-dip spectroscopy is very similar to that of the UV-UV depletion technique. IR-UV hole-burning spectroscopy can also be realized by fixing the IR laser on a certain vibrational transition of one conformer and by scanning the probe UV laser. In this way the REMPI spectrum is recorded in which all the peaks originating from the pumped conformer are strongly reduced in intensity. For this technique, however, a careful selection of the vibrational transition has to be performed, since the chance that two conformers have overlapping IR transitions is greater than for the case of UV vibronic transitions in the UV-UV hole-burning technique.

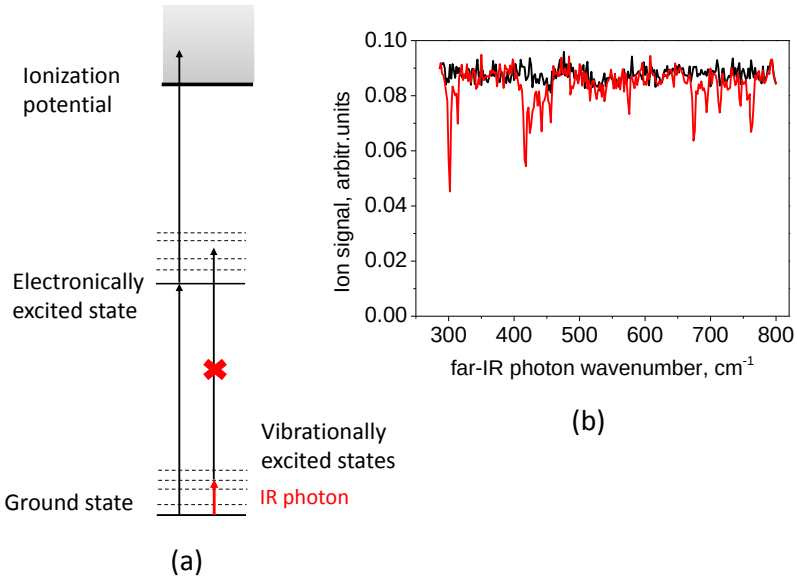

FIGURE 2.5: Principle of the IR-UV ion-dip spectroscopy technique (a), and an experimental IR-UV ion-dip spectrum of *trans* 3-aminophenol (b), shown as illustration of characterystic wavelength-dependent ion-dip signals.

2.5 Free electron laser as a tool for infrared action spectroscopy

The far-IR spectra in this thesis are measured with the help of the IR free electron laser FELIX (Free Electron Laser for Infrared eXperiments) [1]. A free electron laser (FEL) is a special type of laser with unique features. FELs are characterized by high spectral brightness, narrow light bandwidth and continuous wavelength tunability, which makes them highly suitable for various applications. The FELIX light source, for instance, produces tunable, highly intense IR radiation in a broad range of frequencies, allowing accurate measurements of IR absorption spectra in extremely diluted (low-concentration) gas-phase environments.

In conventional lasers stimulated emission of radiation is achieved by creating a population inversion between higher and lower excited states of an active lasing medium. The emitted radiation with a frequency, equal to the difference between these two

states, is amplified in a laser cavity, thus resulting in a coherent laser beam with a narrow bandwidth. To achieve tunability of laser frequency, optical parametric oscillator can be used, which is based on the crystals with high quadratic optical nonlinearity. Also, certain laser media, such as organic dyes or semiconductors, allow tuning wavelength of radiation. Nevertheless, the tuning range is limited to the choice of the certain media. In contrast, FELs does not have a principal limitation for the wavelength of emitted radiation, as the active lasing medium in this case is represented by electrons traveling with relativistic speeds. The electrons propagate through a periodic magnetic field created by an array of magnets with alternating dipoles, called undulator, and perform a wiggling motion due to Lorentz forces, thus emitting radiation. The wavelength of the radiation is given by

$$\lambda = \frac{\lambda_u}{2\gamma^2}(1 + K^2), \tag{2.3}$$

where λ_u is the undulator period, K is a dimensionless parameter proportional to the strength of the magnetic field, and γ is the Lorentz factor

$$\gamma = \frac{1}{\sqrt{1 - \frac{v^2}{c^2}}}. \tag{2.4}$$

Here, v denotes the velocity of electrons, and c is the speed of light. The K parameter is given by

$$K = \frac{eB\lambda_u}{2\pi m_e c}, \tag{2.5}$$

where e is the electron charge, B is the magnetic field strength and m_e is the electron rest mass. As can be seen from equations 2.3-2.5, the wavelength of radiation can be tuned by changing the energy (velocity) of the electrons, and the strength of the magnetic field B. The latter can easily be tuned by changing the gap between the undulator magnets. The undulator period λ_u is usually kept fixed.

The FEL principle allows achieving laser radiation in a very broad spectral range spanning from microwaves to X-rays. The tuning region of the FELIX, for example, ranges from 3 to 150 μm (3200-80 cm^{-1}), which covers the mid-IR, far-IR and partly the THz spectral ranges. Several electron energies are used in this case to cover such a broad range. In this thesis, the typical frequency range used for gas-phase spectroscopy is 220-1800

cm^{-1}. It is achieved by continuous scans from 220 to 800 cm^{-1}, and from 650 to 1800 cm^{-1}, by means of changing the undulator gap, with the electron energy kept fixed for each range.

2.6 Computational: frequency calculations and VPT2 approach

2.6.1 Double harmonic approximation

In order to get valuable information about molecular structure from experimental IR spectra, they have to be compared with theoretical spectra of lowest-energy stable conformations of the molecule. To achieve this aspect, possible structures are prepared by means of conformational search methods [33, 34], and are submitted to the geometry optimization procedure [35], performed with *ab initio* or DFT methods. Geometry optimization is aimed at bringing the molecule to a local energy minimum on a potential energy surface (PES). The next step is to calculate the vibrational frequencies and intensities for the obtained molecular structures, which is usually done within the double harmonic approximation. For a harmonic oscillator the potential energy is described by a parabola $V = \frac{1}{2}kx^2$, where x is the displacement from the equilibrium position and k is the force constant. For a molecule with N atoms we can represent the potential energy by a Taylor expansion, which within the harmonic approximation is truncated at second order

$$V(x_1, x_2, x_3, ...x_{3N}) = V_0 + \sum_{i=1}^{3N} \left(\frac{\partial V}{\partial x_i}\right)_{x_i=0} x_i + \\ + \frac{1}{2} \sum_{i,j=1}^{3N} \left(\frac{\partial^2 V}{\partial x_i \partial x_j}\right)_{x_i=x_j=0} x_i x_j \ + \ldots,$$

where V_0 is a constant, the second term with first derivatives is zero due to optimized geometry (potential energy minimum), and the third term is the force constant:

$$k = \left(\frac{\partial^2 V}{\partial x_i \partial x_j}\right)_{x_i=x_j=0}.$$

Thus, the force constant matrix (Hessian matrix, $3N \times 3N$) is formed from the second-order partial derivatives of the potential.

At the following steps the force constants are converted to mass-weighted Cartesian coordinates $q_i = \sqrt{m_i}x_i$, and the Hessian is diagonalized yielding $3N$ eigenvectors and $3N$ eigenvalues. The square roots of the eigenvalues are the fundamental frequencies of the molecule, with 6 of them equal to zero (3 translational and 3 rotational modes). The remaining $3N$-6 eigenvectors are normal modes, and have the meaning of independent fundamental vibrational motions, for which the center of mass is not moving.

In the same manner the dipole moment can be represented by a Taylor expansion, though in this case it is truncated at first order. The first order derivatives of the dipole moment allow calculating harmonic intensities, corresponding to each normal mode.

2.6.2 Second-order vibrational perturbation theory (VPT2)

The VPT2 approach goes beyond the double harmonic approximation, and takes into account also third- and forth-order derivatives of the potential, and second-order derivatives of the dipole moment [20]. The higher-order derivatives are calculated numerically, which requires evaluation of the Hessian matrices in $6N$-11 spatial points in the vicinity of the PES minimum. The calculated derivatives are then treated as perturbations to the harmonic potential, and this problem is solved by means of second-order perturbational theory. As a result, the anharmonic matrix χ_{ij} is constructed, which allows calculating the fundamental frequencies, corrected for anharmonicity

$$\nu_i = \omega_i + 2\chi_{ij} + \frac{1}{2}\sum_{j=1,j\neq i}^{N}\chi_{ij}.$$

Here, ν_i is the VPT2-corrected fundamental frequency and ω_i is a harmonic frequency. In the same manner the frequencies of overtone and combinational bands can be calculated, together with their anharmonic intensities. The VPT2 approach is part of the quantum-chemistry package Gaussian 09 [36].

Chapter 3

Results and Discussions

3.1 Far-infrared studies of aminophenol isomers

This section is devoted to the studies of far-IR spectra of the aminophenol molecule, based on the results presented in Paper I. The main focus of this work was to investigate the low-frequency vibrations and their corresponding spectral features of the phenyl ring and the two important functional groups, the hydroxyl group (OH) and the amino-group (NH_2). The reason for these studies is that the information on such far-IR vibrations still remains sparse, hindering the effective application of far-IR spectroscopy for molecular structural analysis in general. Strong anharmonicity and a high degree of mode-coupling of low-frequency vibrations is one of the reasons which contributes to this problem, complicating the theoretical description of far-IR spectra. To tackle this issue we used the far-IR spectra measured under cooled gas-phase conditions as a benchmark to evaluate the efficiency of the DFT frequency calculations. The evaluation was performed both for calculations within the double harmonic approximation and within the Second-order Vibrational Perturbation Theory (VPT2). The separate variational treatment was applied for highly anharmonic NH_2 wagging (inversion) vibration.

The experimental far-IR spectra, measured in the range of 220-800 cm^{-1} with the help of IR-UV ion-dip spectroscopy and by employing the free electron laser FELIX, showed a wealth of resolved spectral features, specific for the different aminophenol isomers. First of all, the isomer-specificity has to be adressed. The 2-, 3-, and 4-aminophenol molecules show very different spectra in the region studied, despite having the same functional groups (see Fig. 3 of Paper I). The most obvious differences can be found

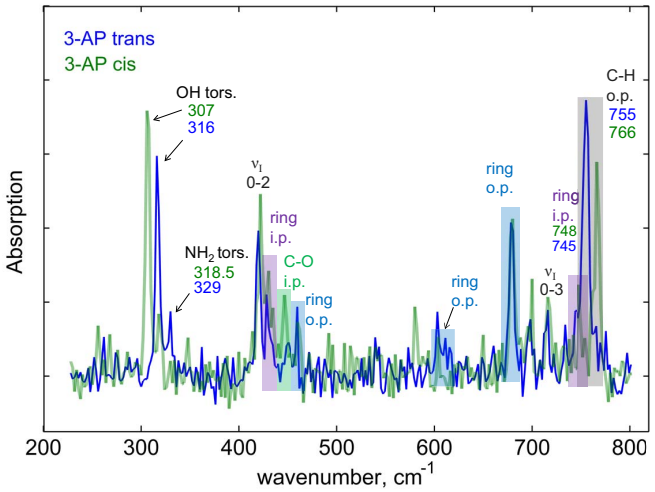

FIGURE 3.1: Experimental absorption spectra of *trans* and *cis* 3-aminophenol in the range of 220-800 cm^{-1}, together with assignments of fundamental vibrational transitions. The ring o.p. transitions are marked in blue, ring i.p. - in pink, C-H o.p. wagging - in grey, C-O i.p. - in green. The vibrational transitions of the NH_2 inversion mode are denoted as ν_I (0-2 and 0-3). Figure is reproduced with permission from [Phys. Chem. Chem. Phys., 2016, **18**, 6275-6283].

in the fundamental transitions corresponding to the phenyl ring out-of plane (o.p.) vibrations, CH o.p. vibrations, and the torsional vibrations of the OH and NH_2 functional groups. These transitions have both different frequencies and intensities for different aminophenol isomers.

As the experimental spectra were obtained in a conformer-selective manner, we were able to study also the differences between the far-IR spectral features of *trans*- and *cis*- 3-aminophenol. Despite the minor differences in the structure (OH group pointing towards or away from the NH_2 moiety), these conformers were distinguished by their far-IR vibrational features (see Fig. 3.1). In this case most of the differences were from the OH and NH_2 torsional vibrations, CH o.p. wagging vibrations, and slightly less difference were observed in NH_2 wagging and CO in-plane (i.p.) bending transitions. In the case of 2-aminophenol molecule, only one conformer was experimentally observed. The measured far-IR spectra strongly supported the assignment to the

TABLE 3.1: Experimentally observed vibrations of 4-aminophenol (4AP), 3-aminophenol (3AP), and 2-aminophenol (2AP), and their assignment. The right-most column outlines the degree of anharmonicity, and the efficiency of the anharmonic VPT2 approach for a particular vibrational motion

Vibration character	Experimental frequencies				Comment about anharmonicity and VPT2 performance
	4AP	trans 3AP	cis 3AP	trans 2AP	
ring breathing	-	745	748	767	weak anharmonicity, VPT2 describes well
CH o.p. wagging	792	755	766	735.5	weak anharmonicity, VPT2 describes well
CCC i.p. bending	759.5	432	434	542	strong anharmonicity except for 4AP, due to NH_2 wag. contribution
	645.5	427	430	486	
	472	-	-	-	
ring puckering	676.5	678	679.5	748.5	high anharmonicity, satisfactory description with VPT2
NH_2 wagging overtone 0-2	467	419	422	437	strong anharmonicity, VPT2 not applicable
CCC o.p. bending	422	612	604	501	weak anharmonicity, VPT2 describes well
	502	459	446	445.5	
CO, CN i.p. bending	326.5	325	312	303	weak anharmonicity, VPT2 describes well
NH_2 torsion	237	329	318.5	323	high anharmonicity, satisfactory description with VPT2
OH torsion	254.5	316	307	286.5	high anharmonicity, satisfactory description with VPT2

trans-conformer, while the *cis* conformer is believed to be much less favorable under the supersonic-jet expansion conditions.

A theoretical modeling of the experimental gas-phase spectra of aminophenol was performed with DFT frequency calculations, both within the double harmonic approximation and with the anharmonic VPT2 approach. It allowed us not only to assign the observed vibrational features, but also to evaluate the accuracy of the most common density functionals and basis sets for the

assignment of far-IR spectra. Such an evaluation was needed in order to find out if conventional DFT frequency calculations can overcome the problems of anharmonicity and non-locality of far-IR vibrational modes for accurate far-IR vibrational assignments. Our study showed that the anharmonic VPT2 approach works reasonably well for the vibrational modes with low anharmonicity and improves the accuracy significantly with respect to the conventional harmonic approximation approach. In contrast, when the anharmonicity or the degree of mode-coupling is very high, such as in the case of the NH_2 wagging vibration, the VPT2 approach did not lead to a satisfactory prediction of frequencies and intensities of the vibrational transitions. Table 3.1 overviews the performance of the VPT2 approach for every vibrational transition observed and assigned in our experiments. The phenyl ring vibrations and CO, CN in-plane bending vibrations, having weak anharmonicity, are described very well by the anharmonic VPT2 approach. The torsional vibrations of OH and NH_2 groups, and the ring puckering vibration have a high degree of anharmonicity, but nevertheless were satisfactory described by the VPT2 approach. The only drawback was that different combinations of density functionals and basis sets produced different anharmonic corrections, with the best accuracy achieved with the functionals B3LYP, B3PW91, B3LYP-D3 and double-zeta basis sets of moderate size.

The strongly anharmonic NH_2 wagging (inversion) vibration required some separate treatment, as the potential energy surface describing this motion has two minima separated by a relatively low barrier [37, 38]. This leads to large tunneling (inversion) splittings of the vibrational energy levels. As a result, several transitions between the tunneling doublet states of the ground state (denoted as 0 and 1) and tunneling doublet states of the first excited state (denoted as 2 and 3) can be observed in the frequency range below 800 cm^{-1}. In order to describe the observed experimental transitions of NH_2 wagging for aminophenol, we applied the model of a double-minimum harmonic well with a gaussian barrier [39] and a variational treatment. In this approach the energy levels are found variationally using the basis set of harmonic oscillator wavefunctions, for the potential energy function in the form

$$V(Q) = \frac{1}{2}\lambda Q^2 + A\exp(-a^2Q^2), \tag{3.1}$$

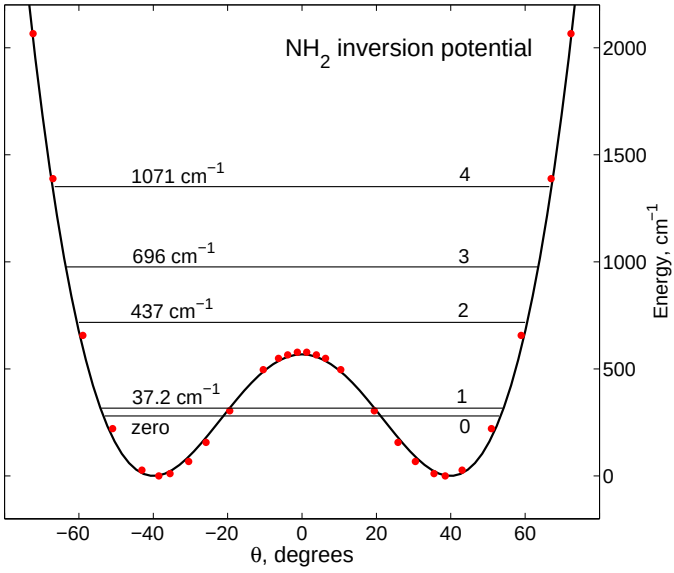

FIGURE 3.2: NH_2 inversion potential of *trans* 2-aminophenol, obtained from an *ab initio* potential energy surface scan (red dots), and by least squares fitting of the *ab initio* and experimental data to the double-minimum potential model with a gaussian barrier (black line).

where Q is a mass adjusted coordinate defined by $2T = \dot{Q}^2$ (T is the kinetic energy of the vibrational motion). By using the experimental frequencies of NH_2 inversion observed for *trans* and *cis* 3-aminophenol, we obtained the parameters of the potential energy function, and the barriers to inversion. In the case of 4-aminophenol and 2-aminophenol, for which less experimental transitions were observed, we applied a different approach. First, we calculated the *ab initio* potential energy profile governing the NH_2 inversion motion by means of a relaxed potential energy scan. Then, a trial potential function (eqn. 3.1) was optimized with the least squares method to best describe the calculated *ab initio* potential energy as well as the frequencies of the 0–2 and 0–3 transitions observed experimentally. The calculated and fitted potential energy curve for trans 2AP is shown in Fig. 3.2, together with the calculated energy structure of the vibrational states. Moreover, *ab initio* data alone used for the calculation of the vibrational energy levels yielded a relatively good agreement with the experimental frequencies as well.

Thus, gas-phase far-IR spectroscopy allowed us to study the low-frequency vibrations of aminophenol, which were found to be isomer- and conformer-specific. The comparison between experimental and theoretical spectra has shown that the far-IR vibrations with moderate anharmonicity and mode-coupling are satisfactory explained by means of the anharmonic VPT2 treatment. For the strongly anharmonic NH_2 inversion vibration, the model of double-minimum potential with a gaussian barrier resulted in a reliable description of the aminophenol experimental spectra.

3.2 Amide IV-VI spectroscopy for peptide structural analysis: the case of Methyl-Acetanilides

In this section the results of Paper II are discussed. Our investigation was devoted to the fundamental far-IR vibrations of a peptide link, the -CO-NH- moiety, in the model peptide molecule MethylAcetanilide. So far, little is known about far-IR vibrations of biomolecules due to their lower absorption cross-sections and more challenging theoretical treatment in comparison with conventional mid-IR studies. However, the delocalized and anharmonic nature of far-IR vibrations carries a wealth of information about the molecular structure. Thus, the extension of the well-established mid-IR spectroscopy to the far-IR and THz ranges will cover all types of molecular vibrations hence revealing precise structural information. Moreover, for large molecules the mid-IR range can suffer from spectral congestion, leading only to families of structures that can be assigned in the experimental spectra. In this case the information acquired from the far-IR spectra can be indispensable. The MethylAcetanilide molecule (see Fig 1.3) has a UV absorption chromophore, a phenyl ring, which enabled us to measure conformer-specific far-IR spectra in the gas-phase. The major advantage of the gas-phase spectra is that they can be directly compared with the results of DFT frequency calculations.

The fundamental vibrations of a peptide link, the so called Amide band vibrations, are illustrated in Fig. 3.3 for the simplest peptide model, N-methylacetamide (NMA). In this work we focus on the Amide IV-VI vibrations, which have frequencies in the far-IR range. The Amide IV vibrations involve CO in-plane

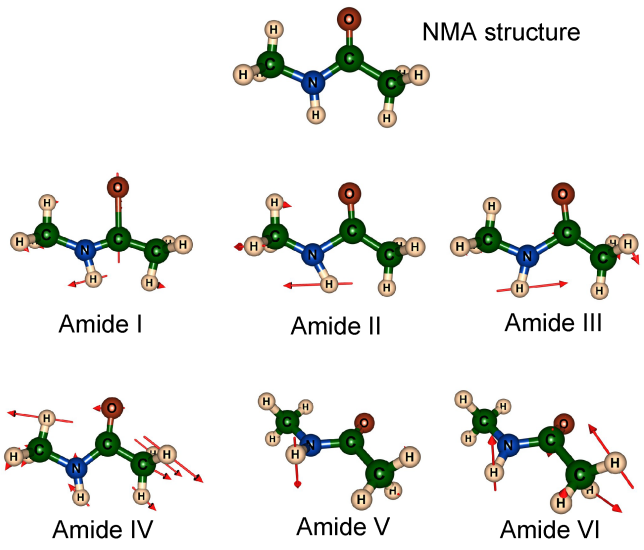

FIGURE 3.3: Graphical representation of the Amide normal modes of N-Methylacetamide (NMA), shown with scaled vectors of the vibrational displacement. The geometry optimization and frequency calculations were performed with B3LYP density functional, and N07D basis set.

(i.p.) bending, as well as the CC stretch and the CNC deformation. Amide V is mostly characterized by the NH out-of-plane (o.p.) bending vibration, and is expected to be strongly anharmonic and very sensitive to hydrogen bonding. Amide VI is referred to CO o.p. bending with some o.p. displacement of the NH group. In the case of the MetylAcetanilide molecule, the Amide IV-VI vibrations can also have contributions from the phenyl ring.

Using the IR-UV ion-dip technique we have studied the mid-IR and far-IR spectra of two isomers of MethylAcetanilide, 2-MA and 4-MA. As an example, the corresponding experimental far-IR spectrum of the observed planar *trans* conformer of 2-MA is shown in Fig. 3.4, together with our theoretical calculations based on the anharmonic VPT2 approach. The experimental and theoretical data obtained in this way revealed several important aspects. First, the calculated spectra are in a very good agreement with the experimental data of the observed conformer, allowing us to assign it to the *trans* geometry, as well as to make a direct vibrational assignment of the observed far-IR bands. Second, as

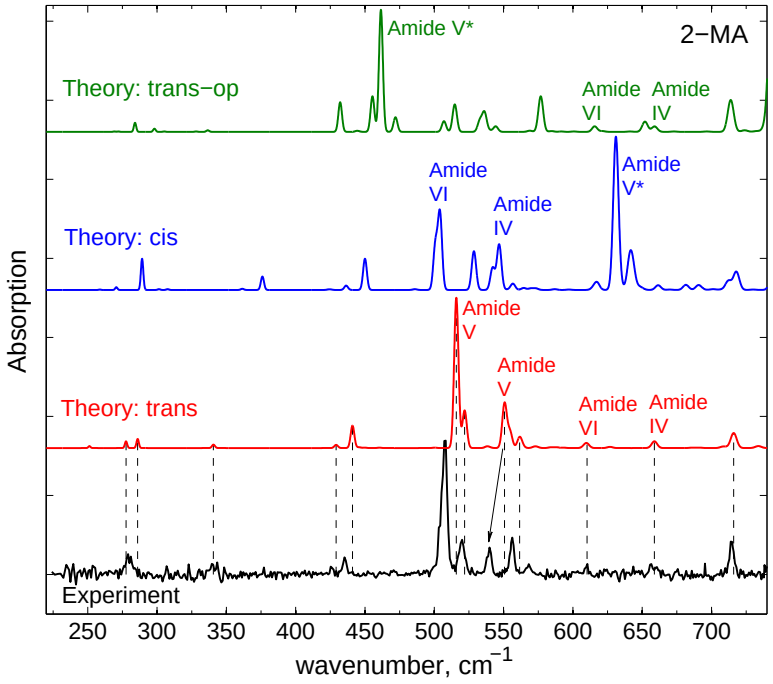

FIGURE 3.4: Experimental far-IR absorption spectra (in black) of the observed conformer of 2-MA, assigned to the planar *trans* structure. The spectra of all possible conformers, calculated with the VPT2 anharmonic treatment at the B3LYP/N07D level of theory, are shown for comparison. The vertical dashed lines denote the position of the fundamental theoretical bands for the *trans* geometry. The marked theoretical NH o.p. bands (Amide V*) were reduced in intensity by a factor of 2.

can be seen from Fig. 3.4, the Amide IV-VI bands are conformer-specific, showing strong differences between the spectra of the possible conformations of 2-MA: planar *trans*, non-planar *trans-op*, and *cis* (see Fig. 1.3). The Amide V, the strongest band, shows the highest sensitivity to the structure of the peptide link. It is predicted to be red-shifted for *trans-op* conformation, and strongly blue-shifted for *cis* conformation with respect to the observed *trans* conformer. The Amide IV and VI bands show the highest sensitivity to the *trans* or *cis* configuration of the peptide link, while in the case of the *trans-op* structure they almost resemble the bands of planar *trans* conformer. Third, we also identified other vibrations involving the peptide link, such as CCO i.p.

bending, CCN deformation, and CNC deformation vibrations. We found that they are not very conformer-sensitive in the case of 2-MA and 4-MA, with exception of some CCN deformation vibrations which showed slight frequency variations for the different conformations (see Table I of Paper II).

Thus, our study of the far-IR specta of MethylAcetanilide revealed that the Amide IV-VI vibrations can be very sensitive to the structure of the peptide link and the molecular backbone. Therefore, far-IR spectroscopy can be an efficient extension to the well-established mid-IR spectroscopy for structural analysis of biomolecules.

3.3 Direct probing of hydrogen bonds by far-infrared spectroscopy

In this section the results of Paper III are discussed. Our study was devoted to the far-IR signatures of the intra-molecular hydrogen bonding (H-bonding) in selected phenol derivatives: cathecol (CAT), saligenin (SLG), salicylic acid (SA), and ethylvanillin (EV). The experimental conformer-specific gas-phase far-IR spectra in combination with DFT frequency calculations allowed us to make an assignment of vibrations which involve the deformations of the hydrogen bonds, and assess their sensitivity to the strength of the H-bonding interaction. The vibrations associated with the H-bonds are depicted in Fig. 3.5, and can be described as: (a) H-bond stretching (or in-plane scissoring of the two H-bonded functional groups), (b) torsional vibration of the H-bonded OH group, and (c) torsional vibration of the free OH group.

The frequencies of the assigned H-bond stretching vibrations are shown in Fig. 3.6a, versus the length of the H-bond donating OH group L_{OH} for each molecule studied. The length of the H-bond donating functional group was chosen as a reliable measure of the H-bond strength [40–42]. As one can see from the figure, the five-membered and six-membered rings closed by the H-bond can be clearly distinguished by means of the frequency of the H-bond stretching vibrations. The range of 300-350 cm^{-1} corresponds to five-membered rings, while the range of 225-260 cm^{-1} to six-membered rings. The H-bond stretching vibration is associated with opening and closing of the H-bonded ring, so its frequency depends on the ring stiffness. When an extra atom is added to the ring in the case of a six-membered ring, the

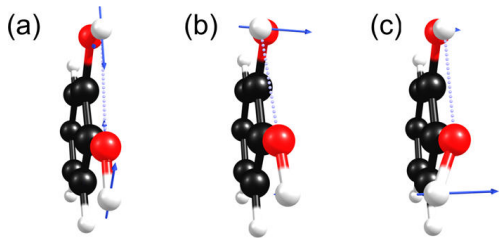

FIGURE 3.5: Vibrational normal modes that involve H-bond deformations, showed for the case of cathecol: (a) H-bond stretching, (b) H-bonded OH torsion and (c) free OH torsion. Carbon atoms are depicted with black spheres, oxygen - with red, and hydrogen with white. This figure is reprinted with permission from [J. Phys. Chem. Lett., 2016, 7 (7), pp 1238–1243].

frequency is red-shifted versus the case of the five-membered rings because the extra atom adds more flexibility to the ring. This reasoning can be extended to the larger H-bonded ring structures. For instance, the frequencies of the H-bonding vibrations for seven and ten-membered rings in dipeptides [22, 23] were observed in the range 100-150 cm^{-1}, well below the range of six-membered rings. Thus, the red-shift of the H-bond stretching frequency directly indicates the increase in the flexibility of larger rings closed by H-bonds.

As can be seen from Fig. 3.6b, the frequencies of the H-bonded OH torsional vibrations increase consistently with the L_{OH}, i.e., with the strength of the H-bond. All experimental points follow the linear behavior, except for the rotamer 1 of salicylic acid, most probably due to the very strong resonance-assisted H-bond [43]. The estimated slope of the linear dependence for the OH torsion frequencies is almost twice higher than the corresponding slope of the mid-IR OH-stretching frequencies, which can also be used to study the H-bonding. This shows the remarkable sensitivity of the H-bonded OH torsion vibrations to the strength of the H-bonding, which thus can be used as a direct probe of this weak interaction in other molecules.

The frequency of the last vibration, the free OH torsion, resulted in a non-linear dependence with respect to the strength of the H-bond (see Fig. 3.6c). We found strong variations between the frequencies of the different structural arrangements of the three molecules studied, for which the H-bond is donated to the

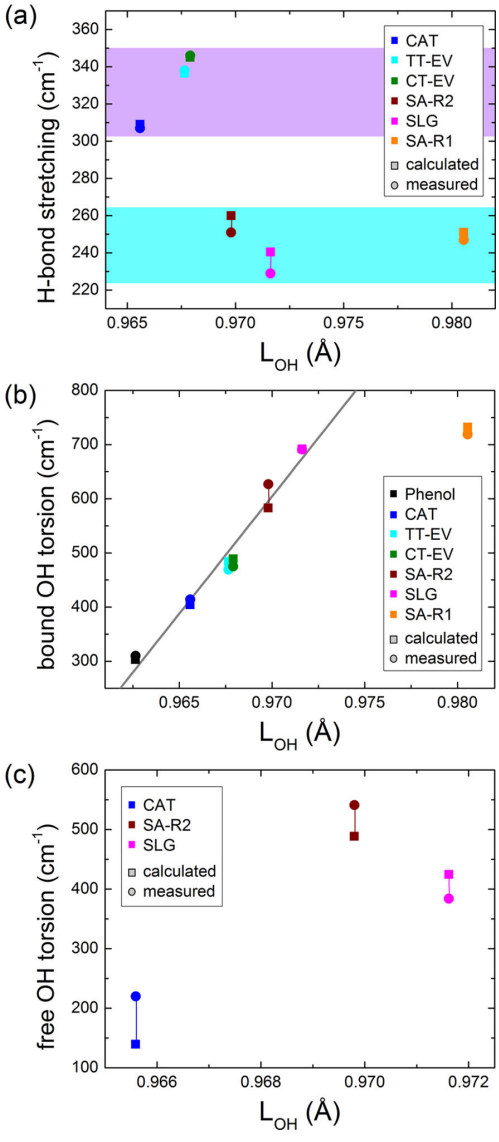

FIGURE 3.6: The frequencies of H-bond vibrations versus the length of the H-bond donating OH group, L_{OH}. The data for the H-bond stretching vibrations is shown in panel (a), the H-bonded OH torsion in panel (b), and the free OH torsion in panel (c). Panel (a) shows the frequency regions corresponding to the five-membered (in purple), and the six-membered (in blue) rings. This figure is reprinted with permission from [J. Phys. Chem. Lett., 2016, 7 (7), pp. 1238–1243].

oxygen atom of the OH group. However, even though such variations can be understood on the basis of the present structures, the hitherto obtained molecular dataset was not sufficient to find a specific correlation of this vibration with the strength of the H-bond.

Thus, we have found two vibrations which allow a direct measure of the H-bond strength and the size of the ring closed by a H-bond. This finding further supports the efficiency of far-IR spectroscopy for molecular structural analysis, especially for the studies of biomolecules stabilized by hydrogen-bonding.

Chapter 4

Conclusions and Outlook

This chapter contains conclusions and future perspectives that can be formulated on the basis of the results obtained in this thesis.

4.1 General

The far-IR spectra of the aminophenol isomers, studied in **Paper I**, gave us extensive information on the low-frequency vibrations of the phenyl ring, and the hydroxyl- and amino-groups. We have shown that the far-IR vibrations with moderate anharmonicity and mode-coupling are satisfactory explained by means of anharmonic VPT2 treatment. Moreover, the model of double-minimum potential with a gaussian barrier resulted in reliable description of the experimental data for the NH_2 inversion transitions of aminophenol. The information obtained for aminophenol can be very useful in the studies of similar aromatic systems, in terms of vibrational assignment, and in terms of theoretical approaches efficient to tackle vibrational anharmonicity.

Our study of fundamental far-IR vibrations of the peptide link, presented in **Paper II**, has shown that Amide IV-VI vibrations have the potential for precise structural analysis of peptide-like molecules. Especially the Amide V bands are very promising, being relatively intense and having frequencies that are very sensitive to the structural arrangement of the peptide link. Moreover, the *trans* and *cis* configurations of the peptide link can be directly characterized by their far-IR spectra in the range of 400-800 cm^{-1} due to the large variations in the corresponding Amide IV-VI bands. This finding can be important for the structural characterization of cyclic peptides, where links of the *cis*-type can be present [44–48].

The study of far-IR vibrations, associated with intra-molecular hydrogen bonds in phenol derivatives (**Paper III**), has revealed two important aspects. First, we have shown that the size of the ring closed by the hydrogen-bond can be characterized by the frequency of the hydrogen-bond stretching vibration. Second, the strength of the hydrogen-bonding interaction can be determined from the frequency of the hydrogen-bonded OH torsional vibration. Far-IR spectroscopy of these vibrations can serve as a direct probe of hydrogen bonding interactions.

4.2 Conformer- and isomer- selectivity of far-infrared vibrations

Gas-phase far-IR spectroscopy combined with quantum chemical calculations, performed in this thesis for various aromatic molecules, have shown that different molecular isomers and conformers have distinct far-IR features that allow precise structural assignment. The isomer-selectivity of far-IR vibrations was observed for the isomers of aminophenol and MethylAcetanilide. The conformer-selectivity was demonstrated experimentally for the 3-aminophenol, ethylvanillin and salicylic acid, for which more than one conformer was observed and assigned. For the other molecules studied only one conformer was observed, but still the distinct far-IR vibrational features enabled unambiguous assignment of the experimental spectra to one of the possible conformations.

4.3 Performance of VPT2 for anharmonic treatment of far-infrared vibrations

In this thesis the VPT2 method was applied for the anharmonic treatment of far-IR vibrations. As gas-phase far-IR spectroscopy allowed a direct comparison between the measured and calculated spectra, we were able to assess the performance of VPT2. This method was found to be reliable for calculations of frequencies and intensities of vibrations with low and moderate anharmonicity, but not applicable for strongly anharmonic vibrations, such as NH_2-inversion. For the vibrations with moderate anharmonicity, the VPT2 method resulted in an almost two-fold increase of accuracy compared with the conventional harmonic approximation. Moreover, VPT2 enabled us to calculate overtone

and combinational transitions, thus assisting the assignment of the experimental spectra. Therefore, the VPT2 approach can be suggested for highly accurate calculations of theoretical far-IR spectra for semi-rigid molecules with low number of strongly anharmonic vibrations.

4.4 Outlook and future perspectives

Firstly, the study of the far-IR spectra of aminophenol (**Paper I**) brought our attention to the strongly anharmonic NH_2-inversion (wagging) vibration. In future, it would be particularly interesting to study this vibration in biological molecules such as peptides and nucleic acid bases, where the NH_2 group is frequently present. In the case of aminophenol, the double-minimum nature of the potential governing amino-inversion motion originated from the two energetically identical equilibrium geometries, with the amino-group hydrogen atoms positioned out-of-plane with respect to the aromatic ring. The amino-groups of biomolecules can be non-planar as well [49], which may lead to similar effects we observed for aminophenol. The presence of hydrogen bonding can lead to a non-symmetric double-minimum potential and even more interesting effects on the far-IR spectra of NH_2-inversion vibration [50].

Secondly, the study of fundamental far-IR vibrations of a peptide link (**Paper II**) has shown that Amide IV-VI bands can be highly sensitive to hydrogen bonding and other weak interactions. Therefore future experimental and theoretical studies on this matter are highly motivated. The expectation from the theoretical data for the hydrogen-bonded dimers of the N-MethylAcetamide is that the frequency of the Amide V band can be blue-shifted by more than 50% compared with the bare molecule. Thus, Amide V bands can provide a very sensitive probe of the strength of the hydrogen bonds, as well as the molecular structure of biomolecules in general.

Thirdly, the far-IR study of phenol derivatives (**Paper III**) has shown that the frequencies of far-IR vibrations of hydrogen-bonded hydroxyl (OH) groups can serve as a direct measure of the strength of hydrogen bonding, as well as the size of the ring closed by a hydrogen bond. This finding, together with the high sensitivity of Amide IV-VI vibrations to hydrogen bonding (**Paper II**), opens new possibilities for structural analysis of biological molecules stabilized by hydrogen bonding interactions.

Finally, IR-UV ion-dip spectroscopy, applied in this thesis, allowed us to measure the far-IR spectra in a conformer-specific manner. However, this technique is limited to molecules that have a UV chromophore. Recently, we have demonstrated a new technique [51], which overcomes this limitation and can measure gas-phase IR spectra of neutral molecules of arbitrary structure. The new technique substantially extends the scope of the molecules that can be studied by IR spectroscopy, and we plan to apply it for the structural analysis of peptides without a chromophore.

Sammanfattning

För att fundamentalt förstå biologiska processer krävs framför allt kunskap om biomolekylers strukturer och svaga inter- och intramolekylära växelverkningar (t ex vätebindningar). Molekylstrukturer och svaga växelverkningar kan direkt studeras med hjälp av långvågigt infraröd (FIR) eller THz spektroskopi genom att undersöka lågfrekvensmolekylära vibrationer. I denna avhandling presenterar jag resultat från både experimentella och teoretiska undersökningar av lågfrekventa vibrationer i små aromatiska och biologiskt viktiga molekyler. För att kunna jämföra experimentella och teoretiska resultat, utförs FIR-spektroskopi på gas med en metod som kan skilja på olika konformer av molekylerna. Mätningar i det infraröda området av molekyler innehållande en peptidlänk (-CO-NH-) avslöjade att lågfrekventa Amide IV-VI vibrationer är mycket känsliga för peptidlänkens struktur, molekylernas huvudkedja samt den inter- och intramolekylära vätebindningsstyrkan. Med hjälp av FIR-spektroskopi av fenolderivatmolekyler identifierade vi vibrationer som kan användas för att undersöka vätebindningsstyrkan samt storleken på en ring bestående av vätebindningar. Dessutom kunde fördelar och nackdelar med konventionella frekvensberäkningar i det infraröda spektrumet utförda med *ab initio* och täthetsfunktionalteori identifieras genom att testa teorin mot experimentella data. Konventionella metoder kunde exempelvis inte reproducera starka icke-harmoniska vibrationer såsom amino-inversion i aminofenol. Istället används en potential-modell med dubbla minima som framgångsrikt beskrev experimentella spektra av aminofenol. Resultaten som presenteras i denna avhandling kan underlätta både tolkningen av FIR-spektra av mer komplexa biomolekyler och för ytterligare framsteg inom lågfrekvensvibrationsspektroskopi för effektivare strukturanalys och studier av svaga interaktioner.

Acknowledgements

First, I would like to acknowledge my supervisor, Vitali Zhaunerchyk, who contributed a lot of his time to my training as a PhD student. Vitali, thank you for your guidance, mentoring and support. This thesis would not be possible without you.

Second, I would like to thank Raimund Feifel, my co-supervisor, who was always ready to support and encourage. I am also grateful for showing me this wonderful opportunity to do a PhD in Sweden in close collaboration with the Netherlands.

Third, I would like to thank Anouk Rijs, my co-supervisor at the FELIX laboratory in Nijmegen, for her guidance in planning our experiments and fruitful discussions. Also, thank you so much for introducing me to the nice science that can be studied with IR action spectroscopy.

I am also very thankful to Daniël Bakker for the introduction to the experimental techniques at FELIX, and to the calculations with Gaussian09. And, of course, it was great fun to work with you together in the lab. I would also like to acknowledge Bin Yan, Sjors Bakels, Arghya Dey and Qin Ong for their support with different matters in the lab.

I am very thankful to Vitali, Raimund and Dag Hanstorp for their valuable suggestions on how to improve the text of this thesis, and Jonas Andersson and Andreas Hult Roos for their help in the translation of the Swedish summary (sammanfattning på svenska). Also, I would like to thank Vel for publishing his LaTeX template at *www.latextemplates.com*.

Furthermore, I am grateful to all past and present colleagues at Level 8 of Forskarhuset here at Chalmers/University of Gothenburg, for interesting discussions about science or anything else, and for creating a stimulating working environment.

And finally, I am very thankful to my family, who has always supported me.

Bibliography

[1] A. van der Meer. "FELs, nice toys or efficient tools?" In: *Nuclear Instruments and Methods in Physics Research Section A: Accelerators, Spectrometers, Detectors and Associated Equipment* 528:1-2 (2004), 8 –14, http://www.ru.nl/felix/.

[2] J. VandeVondele, M. Krack, F. Mohamed, M. Parrinello, T. Chassaing, and J. Hutter. "Quickstep: Fast and accurate density functional calculations using a mixed Gaussian and plane waves approach". In: *Comput. Phys. Commun.* 167:2 (2005), pp. 103 –128.

[3] M.-P. Gaigeot. "Theoretical spectroscopy of floppy peptides at room temperature. A DFTMD perspective: gas and aqueous phase". In: *Phys. Chem. Chem. Phys.* 12 (2010), pp. 3336–3359.

[4] M. Thomas, M. Brehm, R. Fligg, P. Vohringer, and B. Kirchner. "Computing vibrational spectra from ab initio molecular dynamics". In: *Phys. Chem. Chem. Phys.* 15 (18 2013), pp. 6608 –6622.

[5] A. M. Rijs and J. Oomens, eds. *Gas-Phase IR Spectroscopy and Structure of Biological Molecules*. Vol. 364. Top. Curr. Chem., 2015, 1–406, and references therein.

[6] J. A. Stearns, C. Seaiby, O. V. Boyarkin, and T. R. Rizzo. "Spectroscopy and conformational preferences of gas-phase helices". In: *Phys. Chem. Chem. Phys.* 11 (1 2009), pp. 125–132.

[7] M. Rossi, V. Blum, P. Kupser, G. von Helden, F. Bierau, K. Pagel, G. Meijer, and M. Scheffler. "Secondary Structure of Ac-Alan-LysH+ Polyalanine Peptides (n = 5,10,15) in Vacuo: Helical or Not?" In: *J. Phys. Chem. Lett.* 1:24 (2010), pp. 3465–3470.

[8] A. M. Rijs, M. Kabelac, A. Abo-Riziq, P. Hobza, and M. S. de Vries. "Isolated Gramicidin Peptides Probed by IR Spectroscopy". In: *ChemPhysChem* 12:10 (2011), pp. 1816–1821.

[9] N. S. Nagornova, T. R. Rizzo, and O. V. Boyarkin. "Highly Resolved Spectra of Gas-Phase Gramicidin S: A Benchmark for Peptide Structure Calculations". In: *Journal of the American Chemical Society* 132:12 (2010), pp. 4040–4041.

[10] K. Joshi, D. Semrouni, G. Ohanessian, and C. Clavaguera. "Structures and IR Spectra of the Gramicidin S Peptide: Pushing the Quest for Low-Energy Conformations". In: *The Journal of Physical Chemistry B* 116:1 (2012), pp. 483–490.

[11] L. Laaksonen, P. Pyykkö, and D. Sundholm. "Fully numerical hartree-fock methods for molecules". In: *Computer Physics Reports* 4:5 (1986), pp. 313 –344.

[12] R. Woolley and B. Sutcliffe. "Molecular structure and the born—Oppenheimer approximation". In: *Chemical Physics Letters* 45:2 (1977), pp. 393 –398.

[13] G. Rauhut and P. Pulay. "Transferable Scaling Factors for Density Functional Derived Vibrational Force Fields". In: *J. Phys. Chem.* 99:10 (1995), pp. 3093–3100.

[14] P. Sinha, S. E. Boesch, C. Gu, R. A. Wheeler, and A. K. Wilson. "Harmonic Vibrational Frequencies: Scaling Factors for HF, B3LYP, and MP2 Methods in Combination with Correlation Consistent Basis Sets". In: *J. Phys. Chem. A* 108:42 (2004), pp. 9213–9217.

[15] J. Baker, A. A. Jarzecki, and P. Pulay. "Direct Scaling of Primitive Valence Force Constants: An Alternative Approach to Scaled Quantum Mechanical Force Fields". In: *J. Phys. Chem. A* 102:8 (1998), pp. 1412–1424.

[16] C. Fabri, T. Szidarovszky, G. Magyarfalvi, and G. Tarczay. "Gas-Phase and Ar-Matrix SQM Scaling Factors for Various DFT Functionals with Basis Sets Including Polarization and Diffuse Functions". In: *J. Phys. Chem. A* 115:18 (2011), pp. 4640–4649.

[17] Y. Bouteiller, J.-C. Gillet, G. Gregoire, and J. P. Schermann. "Transferable Specific Scaling Factors for Interpretation of Infrared Spectra of Biomolecules from Density Functional Theory". In: *J. Phys. Chem. A* 112:46 (2008), pp. 11656–11660.

[18] R. D. Amos, N. C. Handy, W. H. Green, D. Jayatilaka, A. Willetts, and P. Palmieri. "Anharmonic vibrational properties of CH2F2 : A comparison of theory and experiment". In: *J. Chem. Phys.* 95 (1991), p. 8323.

[19] V. Barone. "Anharmonic vibrational properties by a fully automated second-order perturbative approach". In: *J. Chem. Phys.* 122 (2005), p. 014108.

[20] V. Barone, M. Biczysko, and J. Bloino. "Fully anharmonic IR and Raman spectra of medium-size molecular systems: accuracy and interpretation". In: *Phys. Chem. Chem. Phys.* 16 (5 2014). and references therein, pp. 1759–1787.

[21] T. K. Roy and R. B. Gerber. "Vibrational self-consistent field calculations for spectroscopy of biological molecules: new algorithmic developments and applications". In: *Phys. Chem. Chem. Phys.* 15 (24 2013), pp. 9468–9492.

[22] S. Jaeqx, J. Oomens, A. Cimas, M.-P. Gaigeot, and A. M. Rijs. "Gas-Phase Peptide Structures Unraveled by Far-IR Spectroscopy: Combining IR-UV Ion-Dip Experiments with Born-Oppenheimer Molecular Dynamics Simulations". In: *Angew. Chem. Int. Ed.* 53 (2014), pp. 3663 –3666.

[23] J. Mahe, S. Jaeqx, A. M. Rijs, and M.-P. Gaigeot. "Can far-IR action spectroscopy combined with BOMD simulations be conformation selective?" In: *Phys. Chem. Chem. Phys.* 17 (39 2015), pp. 25905–25914.

[24] L. Pele and R. B. Gerber. "On the number of significant mode-mode anharmonic couplings in vibrational calculations: Correlation-corrected vibrational self-consistent field treatment of di-, tri-, and tetrapeptides". In: *J. Chem. Phys.* 128 (2008), p. 165105.

[25] D. S. Berkholz, C. M. Driggers, M. V. Shapovalov, R. L. Dunbrack, and P. A. Karplus. "Nonplanar peptide bonds in proteins are common and conserved but not biased toward active sites". In: *Proceedings of the National Academy of Science* 109 (Jan. 2012), pp. 449–453.

[26] R. Improta, L. Vitagliano, and L. Esposito. "Peptide Bond Distortions from Planarity: New Insights from Quantum Mechanical Calculations and Peptide/Protein Crystal Structures". In: *PLoS ONE* 6 (Sept. 2011), pp. 1–10.

[27] B. A. Mamyrin, V. I. Karataev, D. V. Shmikk, and V. A. Zagulin. "The mass-reflectron, a new nonmagnetic time-of-flight mass spectrometer with high resolution". In: *Zh. Eksp. Teor. Fiz.* 64 (1973), pp. 82–89.

[28] T. A. Miller. “Chemistry and Chemical Intermediates in Supersonic Free Jet Expansions”. In: *Science* 223:4636 (1984), 545–553, and refs. therein.

[29] D. H. Levy. “Laser Spectroscopy of Cold Gas-Phase Molecules”. In: *Annual Review of Physical Chemistry* 31:1 (1980), pp. 197–225.

[30] M. V. Johnston. “Supersonic jet expansions in analytical spectroscopy”. In: *TrAC Trends in Analytical Chemistry* 3:2 (1984), pp. 58–61.

[31] M. S. de Vries and P. Hobza. “Gas-Phase Spectroscopy of Biomolecular Building Blocks”. In: *Annu. Rev. Phys. Chem.* 58 (2007), p. 585.

[32] R. H. Page, Y. R. Shen, and Y. T. Lee. “Local modes of benzene and benzene dimer, studied by infrared–ultraviolet double resonance in a supersonic beam”. In: *The Journal of Chemical Physics* 88:8 (1988), pp. 4621–4636.

[33] R. Judson, E. Jaeger, A. Treasurywala, and M. Peterson. “Conformational searching methods for small molecules. II. Genetic algorithm approach”. In: *Journal of Computational Chemistry* 14:11 (1993), pp. 1407–1414.

[34] S. R. Wilson and W. Cui. “Conformation Searching Using Simulated Annealing”. In: *The Protein Folding Problem and Tertiary Structure Prediction*. Ed. by K. M. Merz and S. M. Le Grand. Boston, MA: Birkhäuser Boston, 1994, pp. 43–70.

[35] G. Fogarasi, X. Zhou, P. W. Taylor, and P. Pulay. “The calculation of ab initio molecular geometries: efficient optimization by natural internal coordinates and empirical correction by offset forces”. In: *Journal of the American Chemical Society* 114:21 (1992), pp. 8191–8201.

[36] M. J. Frisch et al. *Gaussian 09 Revision D.01*. Gaussian Inc. Wallingford CT 2009.

[37] R. A. Kydd and P. J. Krueger. “The far-infrared vapour phase spectra of aniline-ND2 and aniline-NHD”. In: *Chem. Phys. Letters* 49(3) (1977), p. 539.

[38] R. A. Kydd and P. J. Krueger. “The far-infrared vapor phase spectra of some halosubstituted anilines”. In: *J. Chem. Phys.* 69(2) (1978), p. 827.

[39] J. Coon, N. Naugle, and R. McKenzie. "The investigation of double-minimum potentials in molecules". In: *Journal of Molecular Spectroscopy* 20:2 (1966), pp. 107 –129.

[40] Q. Gu, C. Trindle, and J. L. Knee. "Communication: Frequency shifts of an intramolecular hydrogen bond as a measure of intermolecular hydrogen bond strengths". In: *The Journal of Chemical Physics* 137:9, 091101 (2012).

[41] H.-G. Korth, M. I. de Heer, and P. Mulder. "A DFT Study on Intramolecular Hydrogen Bonding in 2-Substituted Phenols:? Conformations, Enthalpies, and Correlation with Solute Parameters". In: *The Journal of Physical Chemistry A* 106:37 (2002), pp. 8779–8789.

[42] F. Weinhold and R. A. Klein. "What is a hydrogen bond? Mutually consistent theoretical and experimental criteria for characterizing H-bonding interactions". In: *Molecular Physics* 110:9-10 (2012), pp. 565–579.

[43] S. J. Grabowski, ed. *Hydrogen Bonding – New Insights*. Vol. 3. Springer Netherlands, 2006.

[44] D. F. Mierke, T. Yamazaki, O. E. Said-Nejad, E. R. Felder, and M. Goodman. "Cis/trans isomers in cyclic peptides without N-substituted amides". In: *Journal of the American Chemical Society* 111:17 (1989), pp. 6847–6849.

[45] M. T. Oakley and R. L. Johnston. "Exploring the Energy Landscapes of Cyclic Tetrapeptides with Discrete Path Sampling". In: *Journal of Chemical Theory and Computation* 9:1 (2013), pp. 650–657.

[46] S. Wiedemann, A. Metsala, D. Nolting, and R. Weinkauf. "The dipeptide cyclic(glycyltryptophanyl) in the gas phase: A concerted action of density functional calculations, S0-S1 two-photon ionization, spectral UV/UV hole burning and laser photoelectron spectroscopy". In: *Phys. Chem. Chem. Phys.* 6 (10 2004), pp. 2641–2649.

[47] A. P. Wickrama Arachchilage, F. Wang, V. Feyer, O. Plekan, and K. C. Prince. "Photoelectron spectra and structures of three cyclic dipeptides: PhePhe, TyrPro, and HisGly". In: *The Journal of Chemical Physics* 136:12, 124301 (2012), 124301, and refs. therein.

[48] A. G. Abo-Riziq, B. Crews, J. E. Bushnell, M. P. Callahan, and M. S. D. Vries. "Conformational analysis of cyclo(Phe-Ser) by UV–UV and IR–UV double resonance spectroscopy and ab initio calculations". In: *Molecular Physics* 103:11-12 (2005), pp. 1491–1495.

[49] O. Bludsky, J. Sponer, J. Leszczynski, V. Spirko, and P. Hobza. "Amino groups in nucleic acid bases, aniline, aminopyridines, and aminotriazine are nonplanar: Results of correlated abinitio quantum chemical calculations and anharmonic analysis of the aniline inversion motion". In: *J. Chem. Phys.* 105:24 (1996), pp. 11042–11050.

[50] K. H. Hughes and J. N. Macdonald. "Boltzmann wavepacket dynamics of tunnelling of molecules through symmetric and asymmetric energy barriers on non-periodic potential functions". In: *Phys. Chem. Chem. Phys.* 2 (16 2000), pp. 3539–3547.

[51] V. Yatsyna, D. J. Bakker, P. Salen, R. Feifel, A. M. Rijs, and V. Zhaunerchyk. "Infrared action spectroscopy of low-temperature neutral gas-phase molecules of arbitrary structure". In: *Phys. Rev. Lett.* (2016), accepted.

Paper I

Aminophenol isomers unraveled by conformer-specific far-IR action spectroscopy

Paper II

Far-infrared Amide IV-VI spectroscopy of isolated 2- and 4-MethylAcetanilide

Paper III

Far-Infrared Signatures of Hydrogen Bonding in Phenol Derivatives